Superalloys 2004
Edited by K.A. Green, T.M. Pollock, H. Harada,
T.E. Howson, R.C. Reed, J.J. Schirra, and S. Walston
TMS (The Minerals, Metals & Materials Society), 2004

Deformation Mechanisms at Intermediate Creep Temperatures in Rene88 DT

G. B.Viswanathan[1], Peter Sarosi[1] , Michael Henry[2],
Deborah Whitis[3] and Michael Mills[1]

[1] Department of Materials Science and Engineering, The Ohio State University, Columbus, OH, [2] GE Global Research Center, Schenectady NY, [3]Materials and Processes Engineering Department, GE Aircraft Engines, Cincinnati, OH

Keywords: superalloy, creep, dislocations

Abstract

The dislocation substructures developed after small-strain (0.5%) creep at 650°C and 121.6 ksi in Rene 88 DT have been analyzed using conventional and high resolution transmission electron microscopy. Clear differences in creep strength and substructures have been observed for samples heat treated with two different cooling rates from the supersolvus heat treatment temperature. For the more rapidly cooled (400°F/min) microstructure exhibits very low initial creep rates, and deformation microtwinning is the dominant deformation process. For the more slowly cooled (75 °F/min) microstructure, the creep rate is much faster, and isolated faulting of individual secondary γ' precipitates is observed. The detailed mechanisms by which these two mechanisms proceed is discussed, and a possible explanation for the transition in creep mechanism based on the effect of the tertiary γ' volume fraction is also offered.

1. Inroduction

The polycrystalline Ni base superalloy Rene 88 DT has been an important disk alloy for aero-engine applications [1] owing to its good tensile and creep properties, and microstructural stability up to 700°C for extended periods of exposure. Experience indicates that the creep strength of this class of superalloys may depend on a number of interrelated microstructural parameters, including the volume fraction, particle size, distribution, and chemical characteristics of the γ' ($L1_2$ structure) precipitates that are present in a disordered solid-solution FCC γ matrix, along with the grain sizes of both the primary γ' and γ phases [2-4]. This work, which focuses on the creep response of this alloy, is part of a larger effort to provide a more quantitative link between the microstructure and properties for this class of superalloy disk material.

Depending on the alloy and deformation conditions, a variety of mechanisms have been reported as operative in the literature based on transmission electron microscopy (TEM) studies. At lower temperatures, deformation seems to be dominated by APB coupled 1/2[110] unit dislocations shearing the γ' precipitates [5,6]. However, the mechanisms responsible for deformation at higher temperatures is much less clear. At very high temperatures (850-1000°C), climb by-pass and sometimes looping around the precipitates by 1/2[110] matrix dislocations have been observed [7,8]. On the other hand, at intermediate temperatures i.e. 650-800°C (depending on the alloy), deformation can be extremely planar and complex. In this regime, the formation of superlattice stacking faults in the precipitates has been reported. In one of the earliest models to explain this deformation mode, Kear et al. [9] suggested that the shearing of the precipitates occurs by parallel 1/2[112] dislocations that are created by the interaction of two non-parallel 1/2[110] type dislocations. According to Condat and Decamp [10], individual 1/2[110] matrix dislocations dissociate (at the γ/γ' interface) into a double Shockley dislocation of the type 1/3[112] that shears the precipitate and a Shockley of the type 1/6[112] that loops around the precipitate. In this model, the matrix is still sheared by a 1/2<110> dislocation. Other studies {11,12] have reported that faulting occurs in both the precipitates as well as in the matrix. Zhang, et al [12] has suggested that this extended faulting is due to 1/2<110> dislocations that have widely dissociated into double and single Shockley partials, with the dissociation encompassing both matrix and precipitates. Even more recently, Decamps et al. [13] have proposed an alternative mechanism in which the shear in the matrix and the precipitate is accomplished by the uncorrelated movement of Shockley partials originating from a single 1/2[110] dislocation. Finally, based on in situ TEM studies, Kolbe [14] has proposed yet another other shear mechanism involving 1/6[112] Shockley partial motion, and suggested that deformation twinning occurs in Nimonic 105 alloy at higher temperatures (above 760°C).

With regard to the variety of shearing modes apparently operative at intermediate temperatures, there are few systematic studies of the effect of microstructure (γ' precipitate size and volume fraction) on the deformation mechanisms. It is possible that the plethora of mechanisms described above may be due to a sensitivity of the operative mechanisms to detailed features of the microstructure. For instance, in a study of C263 Ni-base superalloy, Manonukul et al. [7] has shown that below a critical γ' particle size that particle cutting occurs, while above this critical size, dislocation pinning and climbing is the operative. The finest-scale precipitate structures (i.e. tertiary precipitates produced during aging) are anecdotally considered to play a particularly important role in creep strengthening. However, the possible effect on the creep mechanisms induced by varying the tertiary γ' size and volume fraction has not been explored in detail. In this work, we have sought to clarify the important creep mechanisms at intermediate temperatures, as well as to establish a link between the precipitate structure and the rate-controlling creep processes. This work has been greatly facilitated by the development of an effective technique for imaging and measuring tertiary γ' size distributions using energy filtered TEM (EFTEM), which is discussed in detail in another paper within this proceedings [15].

2. Experimental Procedures

In this study we have primarily focused on the creep response and associated deformation mechanisms for two different microstructures with varying γ' sizes. Two different average cooling rates, 400°F/min. and 70°F/min. from a supersolvus temperature, were performed to vary the γ' size distribution. These cooling rates are also representative of those that can occur in conventional processing of disk components. Constant load

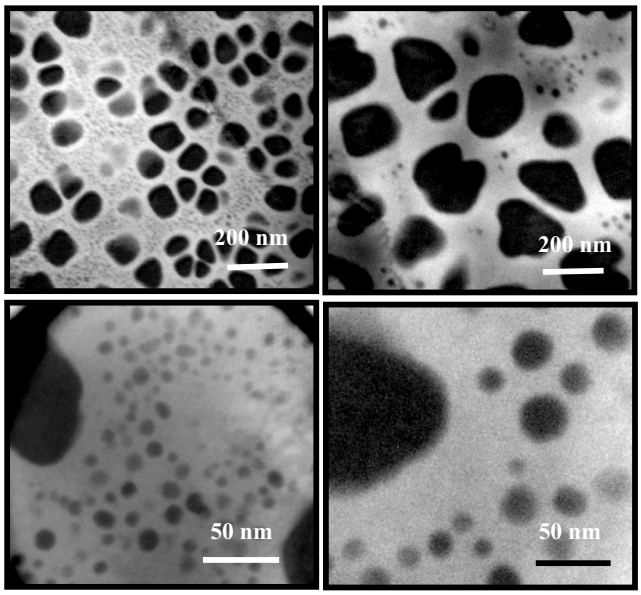

Figure 1. Energy filtered TEM (EFTEM) Cr-map images showing the secondary (upper images) and tertiary (lower images) γ' particles in 400°F/min and75°F/min cooled alloyrespectively.

creep tests were performed in tension at 1200°F and at an applied stress 121 ksi. Creep tests were interrupted at strain levels ranging from 0.2-0.5%, and cooled under load, to enable us to study the deformation substructures through Transmission Electron Microscopy (TEM) analysis. Thin foils for TEM observations were prepared from discs sectioned ~45° to the stress axis of the creep-tested samples. This foil orientation facilitates observation of slip processes on the planes of maximum stress.

3. Microstructure and Creep Behavior

Typical microstructures of the samples cooled at 400°F/min. and 70°F/min from the solutionizing temperature (1150°C) are shown in the EFTEM images of Figure 1 [15]. In the samples cooled at 400°F/min., the secondary and tertiary γ' precipitate sizes were in the range 50-100 nm and 5-20 nm, respectively. In the case of the samples cooled at 75°F/min., the secondary γ' particle sizes were mostly in the range 100-200 nm and the tertiary γ' size was in the range of 12-25 nm. Finally, there was a marked difference in the volume fraction of the tertiary γ' particles for these two microstructures. The 400°F/min. microstructure had a tertiary volume of approximately 12 percent (note that this value does not account for the secondary γ' particles) compared to about 2 percent in the case of 75°F/min. cooled alloy.

Figure 2 illustrates the creep behavior for these two microstructures up until 0.5 % creep strain. The finer structure (400°F/min.) was much stronger than the coarser one (75°F/min.). In both cases, a pronounced acceleration of the creep rate occurs at larger strain, indicating either a dramatic increase in dislocation

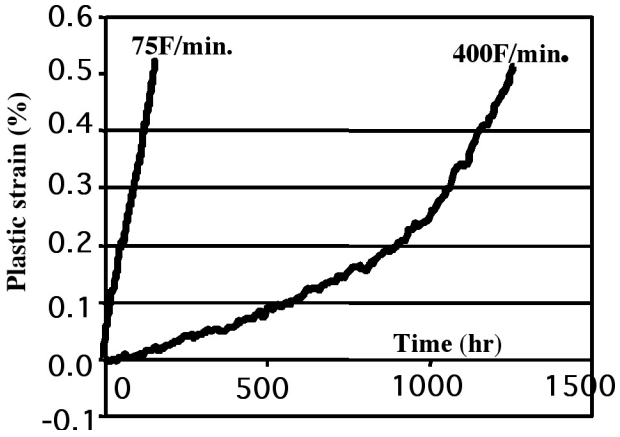

Figure 2. Creep curves showing plastic strain versus time until 0.5% strain for 400F/min. and 75F/min. cooled alloys.

density, a change in the creep mechanism or possible microstructural coarsening. At the applied stress of 121.6 ksi, the time to reach 0.5 % creep strain was ~1250 hours for finer γ' alloy compared to only ~180 hrs for coarser alloy,

4. Deformation Substructures

Investigation of deformation substructures in the TEM has been conducted in these two microstructures, focusing on diffraction contrast TEM analysis of the operative dislocation mechanisms. In the following two sections, the substructures from the finer (400°F/min.) microstructure are described, followed by a discussion of substructures in the coarser (75°F/min.) sample.

4.1 Deformation Substructures For the Finer Microstructure (400°F/min.)

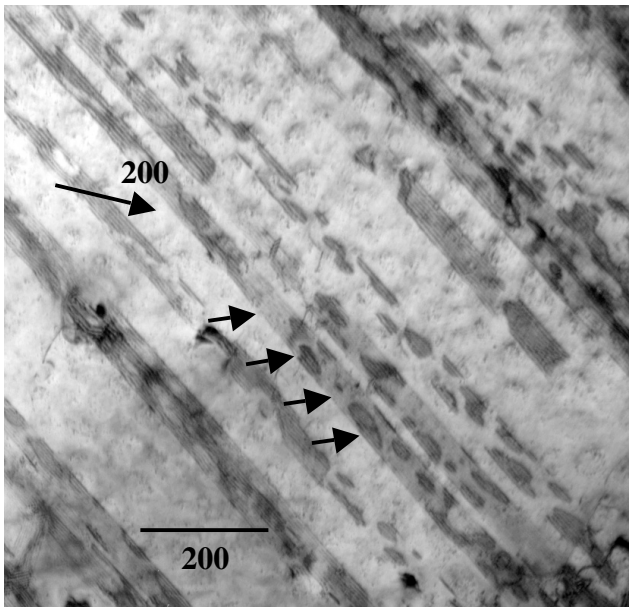

Figure 3 TEM micrograph showing the deformation substructures in sample tested at 1200°F / 121.6 Ksi / 0.5% plastic strain in 400°F/min cooled alloy

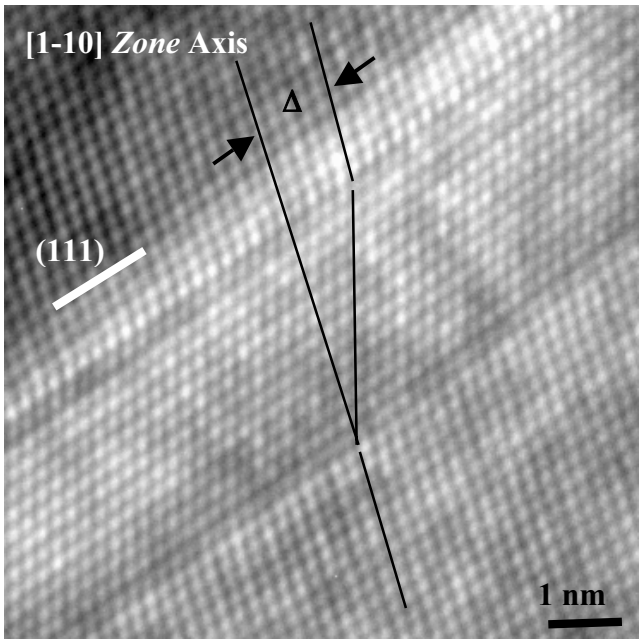

Figure 4 High resolution image revealing these are micro-twins

A representative TEM micrograph for a sample crept of 0.5% strain is shown in Figure 3. The significant observation here is that the deformation is dominated by highly planar, faulted structures that continuously shear the γ matrix as well as γ particles. Aside from these fault features, the dislocation content was minimal in the matrix. Trace analysis has proven that these faults are on {111} octahedral planes. The faults exhibit α-fringe type contrast using fundamental reflections, indicating that they are in fact a fault in the FCC stacking of the matrix. The change in contrast sometimes observed along the length of the faults (e.g. see arrows in Figure 3) indicates the presence of partials on the same {111} plane, or on parallel octahedral planes. Definitive determination of the actual nature of the faults required high resolution transmission electron microscopy (HRTEM). Figure 4 shows an HRTEM image of the fault in the matrix. This image was obtained with the faults edge-on using a [1-10] zone axis for which the (111) fault plane was parallel to the electron beam. This image clearly demonstrates that the faults are indeed twins that extend through the γ matrix and both secondary and tertiary γ' particles. These twins are hereafter referred to as micro-twins since these are very thin, often present as 3-12 atomic planes wide in sample strained to 0.5%.

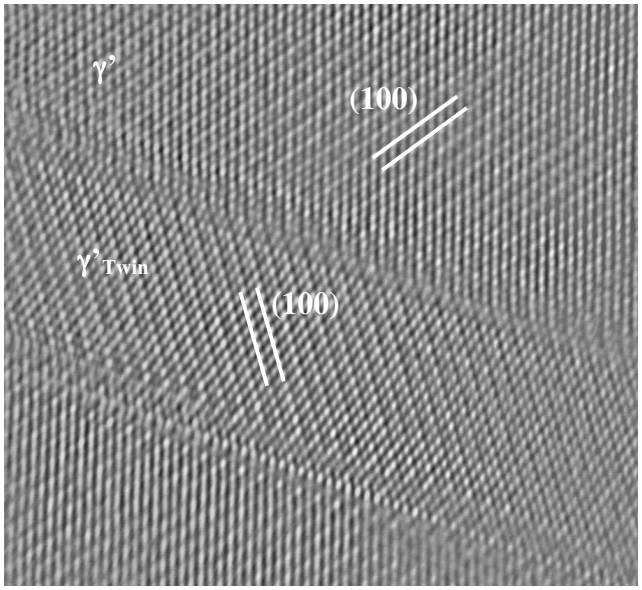

Figure 5 High resolution image revealing micro-twins within γ' precipitate

We can estimate the strain that can be achieved due to the presence of the microtwins, since they provide a permanent marker of the shear displacement. Assuming that the twinning partials are of the type 1/6<112> (see below for an explanation of this assumption), then the displacement due to a single microtwin is given by:

$$\Delta = n\,|b_p| = na_o\left(\frac{\sqrt{6}}{6}\right)^2 \qquad (1)$$

where n is the thickness of the twin, expressed as the number of {111} planes, and a_o is the lattice parameter. The strain due to the twins is then:

$$\gamma = \frac{N_{twin}\Delta_{ave}}{L} \qquad (2)$$

where N_{twin} is the number of twins intercepted by a test line of length L. Given that the HRTEM results indicate n is in the range of 5-10 on average, then the predicted shear strain is between 0.5-1%. Recalling that the macroscopic creep strain for this sample is 0.5% axial strain, this estimate indicates that the microtwinning process can readily account for the majority of the creep strain. This result is consistent with the fact that very little other deformation activity is observed in this sample. Additional HRTEM investigation (Figure 5) has demonstrated that the twinned regions that pass through the secondary γ' particles retain

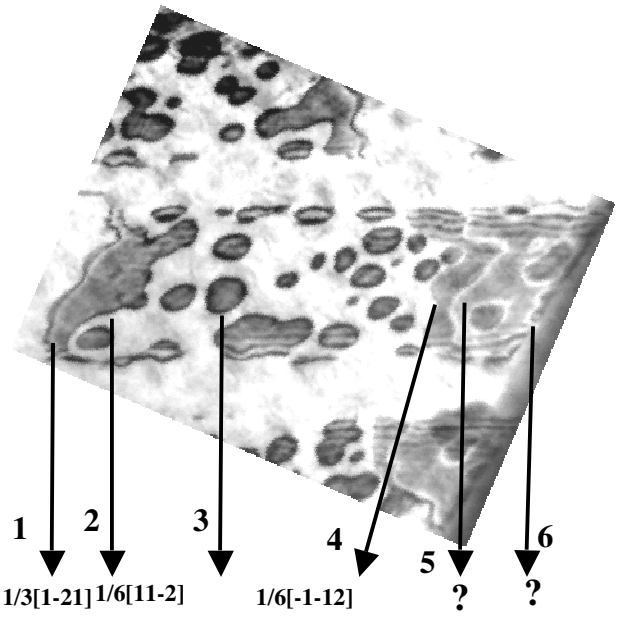

Figure 6. BF TEM micrographs showing early stages of micro-twin formation where the fault plane is imaged in inclined fashion.

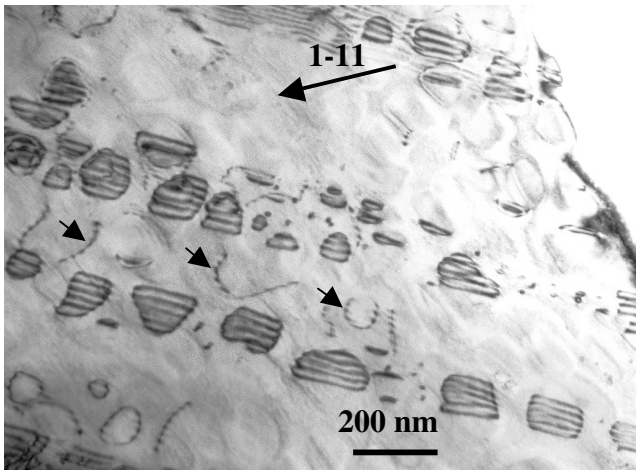

Figure 7. Deformation substructures in sample tested at 1200°F / 1211.6 Ksi / 0.5% plastic strain in 75°F/min cooled alloy:

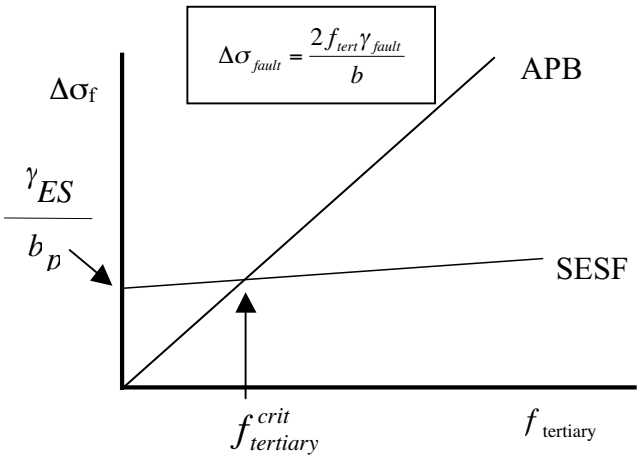

Figure 8. Schematic showing the incremental stress required to shear a coherent particle versus the volume fraction of tertiary γ' . Suggests the existence of mechanism change as function of tertiary volume fraction

the ordered $L1_2$ structure.

Conventional diffraction contrast experiments were undertaken in the TEM to elucidate the nature and character of the twinning partials. An early stage of microtwin formation is captured in Figure 6, in which a microtwin can be seen emanating from the boundary on the right side of the micrograph. The result of our contrast analysis indicates that the twins initiate with the movement on the (111) plane of a lead partial dislocation (labeled as 1), which has the burgers vector of 1/3[1-21]. The dislocation trailing the initial, continuous fault (i.e. dislocation 2) has a burgers vector of 1/6[11-2]. An interpretation of this structure is that it is a unit dislocation that has dissociated into the observed partials according to the reaction:

$$1/2[1\text{-}10] = 1/3[1\text{-}21] + 1/6[11\text{-}2] \qquad (3)$$

The 1/3[1-21] partial dislocation when propagating creates a stacking fault (SF) in the matrix and a superlattice stacking fault (SSF) in the precipitate. This is the region between the dislocations marked 1 and 2 in Figure 6, which shows the fault contrast. The trailing partial marked 2 is a 1/6[11-2] Shockley partial, which removes the stacking fault in the matrix, and creates APB's in the tertiary γ'. This is the reason there is no fault contrast in the matrix behind the dislocation marked 2. However, creation of APB's in the larger secondary γ' precipitates is not energetically favorable, and hence 1/6[11-2] partials (indicated as dislocation 3 in Figure 6) loop around the secondary γ'. As a result, a field of faulted (and looped) secondary precipitates remains in the wake of the lead dislocation group (dislocations 1 and 2). Note that as a result of this rather convoluted process, the formation of APB's is avoided in the larger γ' particles.

The growth of the microtwin from this origin (i.e. the structure associated with dislocations 1-3) to a multiple layer fault is again complex. Twin thickening apparently begins with the passage of the dislocations marked 4, 5 and 6. These dislocations are, presumably, traveling on planes adjacent to the leading set, although this has yet to be definitively proven via HRTEM investigations. Contrast analysis has shown that the dislocation marked 4 is another Shockley partial similar in magnitude to that of dislocations marked 2 and 3 but with opposite sign. Therefore, the Shockley dislocation marked 4, has the burgers vector of 1/2[-1-12]. As this Shockley partial sweeps over the same plane that dislocation 2 has traversed, it is able to annihilate the 1/6[11-2] loops that surround the secondary γ' particles *and* convert the APB's in the tertiary particles back to SSF's. In the matrix, a SF would trail behind dislocation 4. So, the state of shear following dislocation 4 is *identical* to that following dislocation 1, the structure having been sheared by a net displacement of 1/3[1-21]. Unfortunately, dislocations 5 and 6 are difficult to characterize because of the interference from the fault below. However, contrast experiments conducted on a mutilayer microtwin from another grain (not shown here) indicate that the twinning partials have the *same* burgers vector having a direction along <112>. Based on our present data, the twinning partials appear to have burgers vectors of the type 1/6<112> (rather than 1/3<112>), although further detailed contrast analysis is required to validation. Thus, we conclude that microtwin formation is probably a two-step process. In the first step, the shear of the matrix and the precipitate is accomplished by the passage of a 1/3<112> type partial dislocation, followed by a 1/6<112> partial (that together equal a 1/2[110] matrix dislocation). Subsequent shear by twinning appears to be achieved by the motion of identical 1/6<112> Shockley partials on successive {111} planes.

4.2 Deformation Substructures For the Coarser Microstructure (75°F/min.)

The deformation substructure at this applied stress is again dominated by the stacking faults as shown in Figure 7. The faults in the coarser structure are not necessarily nucleated on the grain boundary, nor do they travel the whole length of the grain. Instead they are distributed within the grain in an isolated fashion, and are therefore referred to as isolated faults. Figure 7 shows that the fault contrast is seen only in the sheared precipitates while fault contrast is absent in the matrix. In most instances, these isolated faults shear the γ' particles, leaving dislocation loops around the particles. Burgers vector analysis has determined that these loops are Shockley partials with **b**=1/6[11-2]. The matrix dislocations that are adjacent to the fault (marked in Figure 7) have been characterized to be individual 1/2[110] dislocations that show no apparent tendency for pairing (with another 1/2<110> dislocation), nor for dissociation into partial dislocations.

5. Discussion

In this study, the temperature and stress have been kept constant, and the effect of γ' size on the creep behavior has been the focus. In view of the deformation substructures just described, we now attempt to rationalize the creep behavior of these two microstructures by proposing viable creep mechanisms. At the outset, it should be emphasized that a common thread for all the substructures examined in this study is the remarkable planarity of slip. On this basis, the operation of climb by-pass of particles by dislocations does not appear to be prevalent under the present conditions at 650°C, although this process certainly may become important at elevated temperatures. In addition, at the relatively small strain levels examined presently, the substructures observed in a given grain were typically associated with the operation of a single slip system. Thus, the mechanism previously proposed by Kear, et al [9] to explain faulting of the precipitates is clearly not appropriate for the present case.

5.1 Mechanisms in the Coarser Structure (75°F/min.)

The dominant deformation mechanism in the alloy containing coarser γ' precipitates is isolated faulting of the secondary γ' precipitates. Our TEM studies have determined that the substructures consist of faulting mostly in the precipitates and not in the γ matrix, while the precipitates are looped by 1/6<112> Shockley partial dislocations. Several researchers [9-13,16] have reported similar observations. The present results can be explained by the mechanism originally proposed by Condat and Decamps [10]. In this model, 1/2<101> dislocations are present in the matrix, while the precipitates experience a net shear of 1/3[112]. This is accomplished in the following sequence. A 1/2[-101] dislocation enters the precipitate, dragging an APB behind it. Due to the high energy of this fault, at some stage it becomes energetically favorable to nucleate a Shockley partial loop on the (111) plane of the APB, thereby converting the APB into a much lower energy superlattice stacking fault (SSF). This process also converts the 1/2[-101] dislocation into a 1/3[-211] super-Shockley partial, via the reaction:

$$1/2[-101] + 1/6[1\text{-}21] \rightarrow 1/3[-211] \quad (4)$$

that can readily sweep across the precipitate, which is then looped by a 1/6[-12-1] dislocation (i.e. "negative" of the dislocation that reacted with the leading 1/2[-101] dislocation). Effectively, the nucleation of the Shockley partial loop within the precipitate allows the matrix to be sheared by a unit 1/2[-101] dislocation, while forming a low energy SSF fault in the precipitate. In should be emphasized that the operation of the 1/2[-101] dislocation in the matrix necessarily means that the tertiary γ' particles *are* being sheared by this translation, thereby forming APB's in these fine precipitates. As initially proposed by Mukherji et al [15], the nucleation of this transforming partial dislocation within the secondary γ' may be the rate limiting process for this deformation mode.

5.2 Mechanisms in the Finer Structure (400°F/min.)

There have been a few earlier studies [17] in which mechanical twinning has been presumed to occur during high temperature tensile testing of Ni-base superalloys. In those cases, the strain rates were much higher than the creep strain rates observed in this study. In this work, we have clearly established that deformation starts with microtwinning in the early stages of creep, and that it is the dominant deformation mechanism at lower stress levels.

We have also described our results that indicate that the processes of microtwin initiation and thickening occurs by the motion of distinctly different partial dislocations. With regards twin initiation, it should be noted that secondary γ' shearing by dislocations 1 through 3 (see Figure 5) is fundamentally the same as the structure identified recently by Zhang et al. [12] as that resulting from the dissociation of a unit matrix dislocation via Equation 3 above. However, the importance of this configuration as the initiator of the microtwinning process was not noted in this previous work. While this might reflect the fact hat microtwinning was not operative in this previous study, it is also possible that the connection between the lead configuration and the subsequent thickening of the twins was not made.

The thickening of the microtwins from this origin appears to be achieved by the motion of **b**=1/6<112> Shockley partials on successive (111) planes, although this hypothesis still requires additional, detailed TEM study which is in progress. Recently, shearing of the γ' precipitates by **b**=1/6<112> Shockley dislocations has been discussed by Kolbe [14]. Motion of **b**=1/6<112> Shockley partials on successive (111) planes would create a high energy (CSF on the habit plane of the twin) and a pseudotwin in γ' ($L1_2$) precipitate. The structure within the pseudotwin would no longer be $L1_2$, but rather a lower symmetry orthorhombic structure with numerous, unfavorable nearest-neighbors. If these Shockley partials move on successive planes, upon entering the precipitate, the CSF can be annihilated and the $L1_2$ structure can be restored by a sequence of diffusion steps among atoms behind the moving dislocations [16]. Since this diffusion process will be easier at higher temperatures, Kolbe has argued that microtwinning by Shockley partial dislocations could be the rate-controlling creep process.

It is not presently possible to definitely associate the rate-limiting process in this regime as that associated with microtwin initiation or thickening. However, it is quite clear that microtwinning is the dominant deformation process operative. This is a remarkable result considering that deformation twinning is conventionally associated with low temperature and high stress conditions, while we have observed twinning for the microstructure and stress level producing the lowest creep rates measured in this study.

5.3 Transition in mechanisms between coarse and fine microstructures

One of the most important results of the present work is that there exists a clear transition in mechanism as a function of microstructural scale. In considering the reason for this transition, and noting that the volume fraction for the tertiary γ' is significantly different for the two microstructures, while that for the secondary γ' is relatively similar, we presently hypothesize that it is the finer tertiary γ' size that determines this transition. The fundamental difference between the two deformation modes is that for isolated faulting, 1/2<110> dislocations are present in the matrix, while for microtwinning, the leading dislocation is a 1/3<112> partial. Therefore, in the former mode, APB's must be created in the tertiary γ' particles, while in the latter mode, SESF's are created in the tertiary γ'. The stress required to shear a coherent particle varies roughly as $2f\gamma/b$, where f is the particle volume and γ is the energy of the fault created in the particle [18]. A qualitative plot of the stress increment required for shearing the tertiary γ' precipitates as a function of the tertiary γ' volume fraction is shown in Figure 8. At small tertiary volume fraction, the matrix and tertiary particles can be sheared by 1/2<110>

dislocations at relatively smaller stress levels since no fault is created in the matrix.. Conversely, at high tertiary γ' volume fraction, shearing by the 1/3<112> dislocation is favored since the energy of the SSF created in the precipitates is much smaller than the energy of the APB's that would be created by the 1/2<110> dislocations. Consequently, we can qualitatively rationalize a transition in deformation mode on this simple, physical basis.

Conclusions

(i) Constant load creep tests have been conducted in Rene'88DT alloy for two different microstructures with varying γ' size obtained by varying the cooling rates from the supersolvus temperature. The finer microstructure (cooled at 400°F/min.) exhibited significantly lower creep rates relative to the coarser structure (cooled at 75°F/min.) when tested at the same stress level and temperature.

(ii) Detailed dislocation analysis indicate that in the finer γ' microstructure the dominant deformation mode is microtwinning. Based on the TEM evidence it is proposed that microtwinning mechanism is a two-step process. Initiation of the twin starts primarily from the dissociation of a/2[1-10] unit dislocation according to 1/2[1-10] = 1/3[1-21] + 1/6[11-2]. The 1/3[1-21] double Shockley (a twinning partial for the $L1_2$ structure) shears the precipitate and the matrix creating stacking faults in both of them and the 1/6[11-2] single Shockley loops around the precipitate. Twin thickening appears to be accomplished by the movement of 1/6[112] type Shockley partial dislocations on successive (111) planes.

(iii) In the coarser microstructure, the dominant deformation mode is isolated faulting. Based on the TEM evidence it is proposed that 1/2[110] unit dislocation initiates the shearing process in the matrix. Shearing in γ' is accomplished by 1/3[112] double Shockley dislocation which is the product of the interaction between 1/2[110] unit dislocation and a 1/6[112] Shockley dislocation that nucleates within the γ' precipitate.

(iv) The transition from the isolated faulting mechanism in coarser γ'microstructure to microtwinning mechanism in the finer γ'microstructure is attributed to the effect of the volume fraction of the tertiary γ' precipitates on the stress required to drive dislocations through the matrix and tertiary particles.

Acknowledgement

Support for this work under the DARPA Accelerated Insertion of Materials (AIM) Program is gratefully acknowledged.

References

1. S.T. Wlodek, M. Kelly and M. Alden., *Superalloy*, (1996), ed. R.D. Kissinger, D.J. Deye, D.L. Anton, A.D. Cetel, M.V. Nathal, T.M. Pollock. and D.A. Woodford: 120-136.
2. N.S. Stoloff," Fundamentals of strengthening" in Superalloys II, ed. C.T. Sims, N.S. Stolofff and W.C. Hagel, John Wiley and Sons, New York, NY, (1987), 61-96.
3. J.R. Groh J.R. *Superallous 1992*, Proc. of the International Symposium at Seven Springs, PA. USA, ed. R.D. Kissinger, D.J. Deye, D.L. Anton, A.D. Cetel, M.V. Nathal, T.M. Pollock. and D.A. Woodford: TMS-AIME
4. J. Schirra. *Superallous 1992*, Proc. of the International Symposium at Seven Springs, PA. USA ed. R.D. Kissinger, D.J. Deye, D.L. Anton, A.D. Cetel, M.V. Nathal, T.M. Pollock. and D.A. Woodford:.TMS-AIME.
5. G.R. Leverant and B.H. Kear , Met.Trans., 1970, 1, 491-98.
6. W.W. Milligan, S.D. Antolovich, " Yielding and deformationbehavior of the single crystal superalloy PWA", "Metal. Trans.A", (1987),18A, 85-95
7. A. Manonukul, F.P.E. Dunne and D. Knowles,"Physically-based model for creep in Ni-base superalloy C263 both above and below the gama solvus,"Acta. mater., 50(2002),2917-2931.
8. Caron P., Henderson P.J., Khan, T and McLean M., Scr. Metall. (1986), 20, 875
9. Kear B.H., Oblak J.M. and Giamei A.F., Metal. Trans A (1970), 1, 2477-2486
10. Condat M. and Decamps B., Scr. Metal., 1987, 21, 607.
11. Milligan W.W. Antolovich S.D., *Metal. Trans. A*, (1991), 22A, 2309-2318.
12. Zhang, Y. H.; Chen, Q. Z.; Knowles, D. M. *Materials Science and Technology* (2001), 17(12), 1551-1555.
13. Decamps B., Raujol S., Coujou A., Sturmet P.S., clement N., Locq D. and Caron P,"On of γ' precipitates by a single (a/6)·[112] Shockley partial in Ni-based superalloys. "Phil. Mag.A, 84(1), (2004), 91-107.
14. Kolbe M. *Materials Science and Engineering*, (2001), A319-321, 383-387.
15. Peter Sarosi[1], G.B. Viswanathan[1], Deborah Whitis[2] and Michael Mills[1], "Imaging and characterization of γ' precipitates in nickel-based superalloys", In this proceedings (2004)
16. Mukherji D., Jiao F., Chen W. and Wahi R. P., *Acta metall. mater*. (1991) 39(7), 1515-1524
17. Dermarker S. and Strudel J.L., "High temperature deformation modes in Ni-base superalloys" Proc. ICSMA 5, "ICSMA 5"eds. P. Hassen, V. Gerold and G. Kostovz., Pergomon Press,1 (1979), 705-710.
18. Dieter G.E. *Mechanical Metallurgy*, Mcgraw-Hill book company, London 2001.